A Laboratory Study on Reduction of the Heat Island Effect of Asphalt Pavements

Bao-Liang Chen[1], Sankha Bhowmick[2], and Rajib B. Mallick[3]

Abstract

Heat islands are formed as a result of construction that replaces vegetation with absorptive surfaces. Air temperature rises as a result of formation of heat islands. One suggested method to reduce the emitted heat from asphalt pavement surfaces is to reduce the temperature of the surface by flowing a suitable fluid through the pavement. The heated fluid could then be used for different end applications. Laboratory experiments were carried out using compacted hot mix asphalt samples with quartzite and metagranodiorite aggregates. Pipes with different surface area were used to flow water through the samples, and the processes were modeled using finite element method. The results clearly show the feasibility of the proposed method, and indicate the beneficial effects of higher thermal conductivity of aggregates and larger surface area of pipes. Velocity and thermal profiles of water in the pipe inside asphalt pavement are analyzed, and the necessity of good contact between asphalt mix and fluid carrying pipe is illustrated.

Key Words: Heat Island, Temperature, Thermal Conductivity, Asphalt

[1] Graduate Research Assistant, Civil and Environmental Engineering, Worcester Polytechnic Institute (WPI), 100 Institute Road, Worcester, MA 01609, Phone: (917) 476-1202 Fax: (508) 831-5808, e-mail:rickchentt@gmail.com (Oral Presentation)
[2] Associate Professor, Mechanical Engineering, University of Massachusetts Dartmouth, 285 Old Westport Road, North Dartmouth, MA 02747, Phone: (508) 999-8619 Fax: (508) 999-8881, e-mail: sbhowmick@umass.edu
[3] Associate Professor, Civil and Environmental Engineering, Worcester Polytechnic Institute (WPI), 100 Institute Road, Worcester, MA 01609, Phone: (508) 831-5289 Fax: (508) 831-5808, e-mail: rajib@wpi.edu

Introduction

Heat islands are formed as vegetation is replaced by asphalt and concrete for roads, buildings, and other structures, which absorb - rather than reflect - the sun's heat, causing surface temperatures and overall ambient temperatures to rise (1). The heat from asphalt pavements is a major contributor to the rise in temperature in areas with asphalt pavements, resulting in what is known as the Urban Heat Island Effect (2). The urban heat island effect is created by the high absorptivity of the pavement surface which subsequently leads to an elevated surface temperature and therefore higher emission from the pavement (3).

Asphalt pavements get heated up by solar radiation, and numerous studies have been conducted on evaluation of temperature profiles inside asphalt pavements, and the effect of different parameters on such temperature (4-15). Because surface radiation follows the Stefan-Boltzmann equation, which involves the fourth power of temperature, a slight increase in the surface temperature results in a significant increase in the emitted heat. This leads to significant increase in energy consumption in order to maintain comfort level. Additionally, studies have shown that air quality also deteriorates under increased temperature due to the heat island effect (16).

Various techniques have been proposed to lower the heat island effect. For asphalt pavements, one prominent method proposed is to use specialized reflective coating so that the albedo is significantly increased (17). This approach has allowed significant lowering of surface temperature. Increased surface reflectivity may increase visibility problems during the daytime. Also, there is a possibility that the reflected light may be absorbed by other surfaces. Therefore, further studies are required to optimize the pavement thermal features for reduction of heat island effect.

One approach being experimented by our group is to use a piping network below the surface of the asphalt pavement. By flowing an appropriate fluid that is cooler than the asphalt mix, we can reduce the temperature of the asphalt pavement surface, while using the heated fluid for different end applications such as heating, power generation or refrigeration. This dual purpose system would require a detailed understanding of the heat transfer characteristics of the asphalt pavement-fluid system and how the different parameters affect the surface temperature of the system.

Background

In our previous work on thermal properties of asphalt pavement materials and heat extraction from pavements (18, 19) we have shown the following:

1. Temperature profiles along the depth of pavements with different structures/subsurface layers are different.
2. Backcalculated thermal conductivity and heat capacity values for similar materials but placed with different base layers are different.
3. Determination of thermal properties of in-place mixes/layers can be made by testing full depth pavement samples under controlled conditions in the laboratory and then using Finite Element method to backcalculate the properties.
4. Use of an aggregate with higher thermal conductivity can significantly enhance the heat transfer efficiency from an asphalt pavement.
5. An effective heat exchanger design is the key in extracting maximum heat from the pavement.

The harvesting of heat energy from asphalt pavements could also be used to lower the surface temperature of pavements and hence reduce the amount of radiated energy. This study was conducted to examine the feasibility of application of this concept.

Objective, Scope, and Approach

The objectives of this study were:

1. Quantify the reduction in pavement surface temperature as a function of flow of water within a pipe

2. Evaluate the effects of different important factors on the heat flow process out of the pavement

In order to develop a fundamental understanding of the heat transfer between the pavement and the fluid carrying pipe system, HMA samples with embedded copper pipe were prepared. A 100W halogen lamp was placed precisely at a given height (for a radiation of 1,000 W/m^2) to simulate solar heating. The approach utilized in this study is shown schematically in Figure 1.

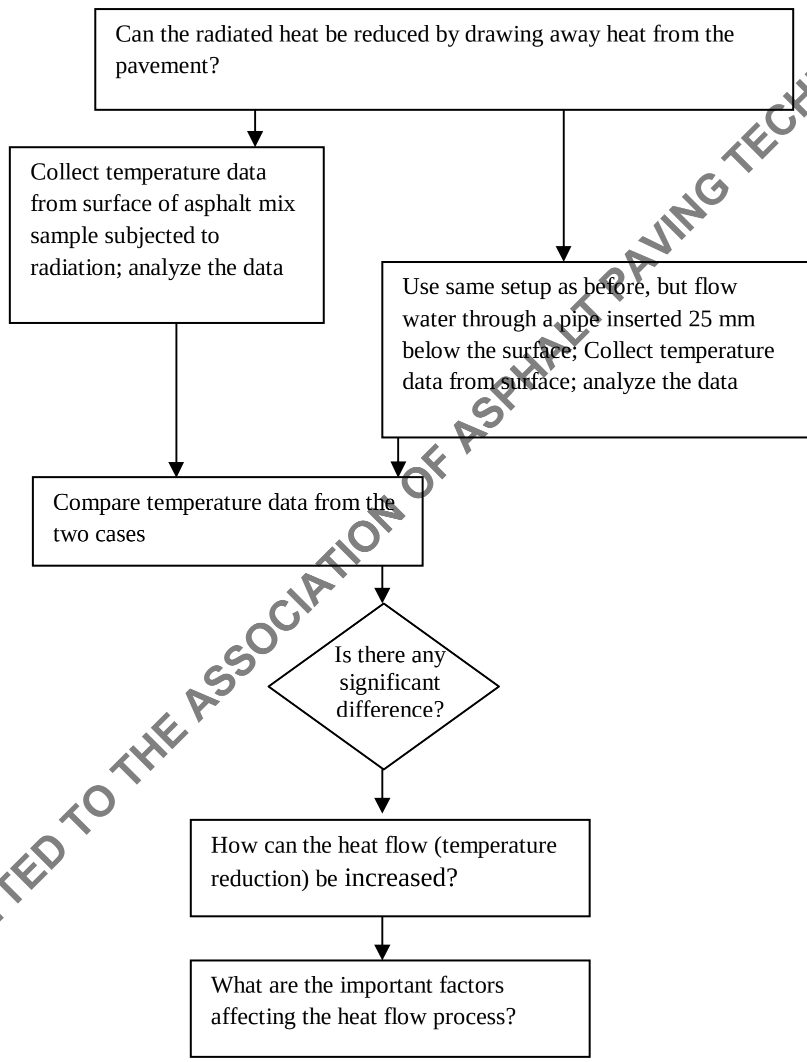

Figure 1 Approach of this study

First, data were collected from samples subjected to radiation, with and without flowing water through inserted pipes. The analysis of the results proved the hypothesis that the reduction in surface temperature can be attained by flowing water in embedded pipes. Based on this result analysis was carried out to understand the effect of the more important factors in maximizing the heat flow out of the pavement (and hence minimizing the radiated heat). The results of these analyses were then validated with further tests.

General Laboratory Test Set Up

The test setup, as described in References 18 and 19, consists of a thermocouple instrumented asphalt mix sample, subjected to radiation from a halogen lamp (Figure 2). Relevant information on thermocouples, data acquisition system and software are shown in Figure 2. A ¼ inch copper pipe was used for flowing water through the asphalt mix sample.

Repeatability of Data

In every case mentioned in the paper three measurements (repetitions) were made. The variability in temperature at different depths of a sample from a repeated set of experiments was found to be very low (example is shown in Figure 3).

Figure 2 Test set up (Note: Thermocouples from Cole-Parmer,Type K (chromel–alumel) thermocouple, −250°C to +482 °C temperature range. Response time is 15 seconds and sensitivity is approximately 41 µV/°C.; Data Acquisition system: National Instruments SC-2345 Series. Software: LabView 8.1

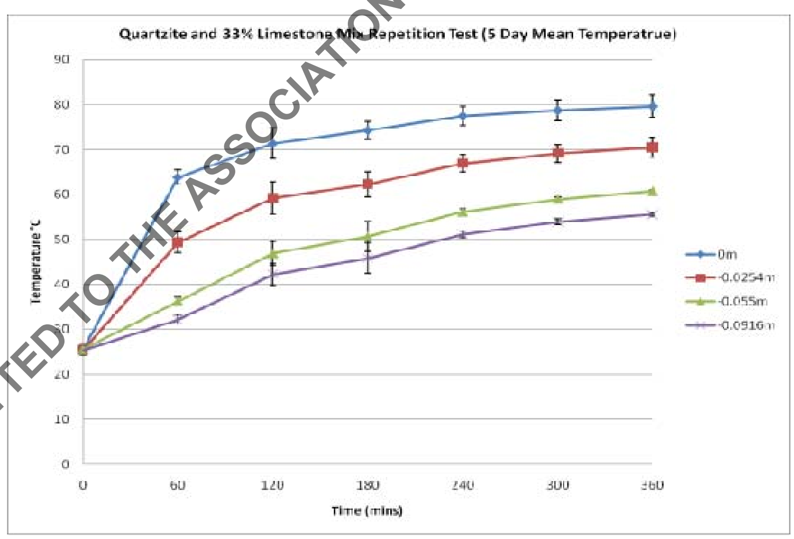

Figure 3 Test data for different mixes

For the asphalt mix used in this part of the study, two types of aggregates were used – a quartzite (consisting of approximately 95% quartz with traces of hematite from New Ulm quarry, MN), and a metagranodiorite (from Wrentham quarry, MA). The asphalt is of PG 64-28 grade. Finite element analysis was conducted using COMSOL (20) software. The quartzite and the metagranodiorite aggregates/mixes are referred to in this paper as Q and M aggregates/mixes, respectively.

The M aggregate was selected as it is a locally available material. The Q aggregate was selected because of its high quartzite content. quartzite aggregate has been reported to have a higher thermal conductivity and heat capacity compared to other aggregates (21). In this study, the thermal conductivity and heat capacities of the Q and the M asphalt-aggregate mixes were estimated from backcalculation of results from heating tests, by comparing the temperature obtained at different depths of samples, with those predicted by Finite Element (FE) analysis (using different "seed" values of thermal conductivity and heat capacity). A FE model of the sample, the location of the thermocouples and a sample plot showing the predicted and experimentally obtained results are show in Figure 4. The thermal conductivity (K) and heat capacity (C) of the Q and M mixes were estimated as follows: Q mix: K= 1.8 W/m·K; C= 1050 J/Kg; M mix: K= 1.2 W/m·K; C= 800 J/kg

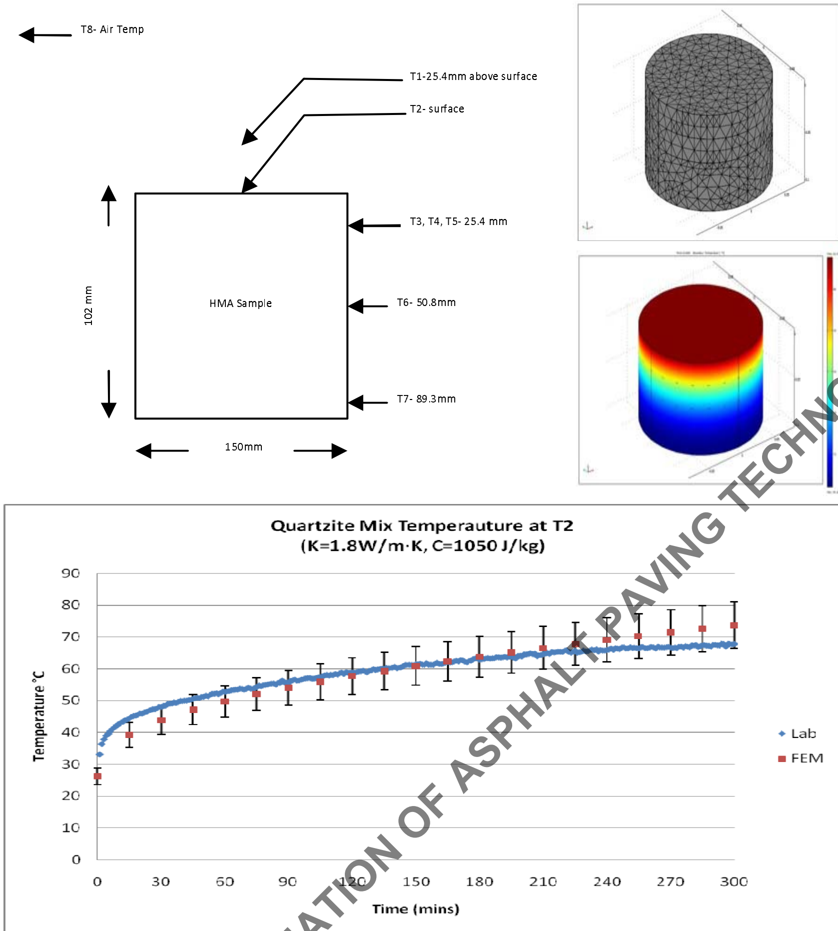

Figure 4 Examples of experimental and FE analysis work for backcalculation of thermal conductivity and heat capacity

Change in Heat Radiation as a Results of Heat Flow

The transfer of energy by electromagnetic waves is called radiation heat transfer. All matter at temperature greater than absolute zero will radiate energy. Energy can be transferred by thermal radiation between a gas and solid surface or between two or more surface. The rate of energy emitted by an ideal surface (black body) with emissivity equal to 1 is given by the Stefan-Boltzmann law:

$$E_b = \varepsilon\sigma T^4$$

Where E_b is the rate of black body radiation energy, ε is the emissivity of the material, and σ = Stefan-Boltzmann constant = $5.68x10^{-8}$ W/(m^2·K^4), and T_s is surface temperature, K.

The emitted radiation intensity from the pavement surface to its surroundings is calculated as

$$q_r = \varepsilon\sigma(T_s^4 - T_{air}^4)$$

Where q_r = emitted radiation, h is heat transfer coefficient, ε is the emissivity of the material, σ = Stefan-Boltzmann constant = $5.68x10^{-8}$ W/(m^2·K^4), T_s is surface temperature in Kelvin, T_{air} is air temperature Kelvin.

The emissivity of a material ε is the ratio of energy radiated by the material to energy radiated by a black body at the same temperature. It is a measure of a material's ability to absorb and radiate energy. A true black body would have the value of ε = 1 while any real object would have ε < 1. Emissivity depends on factors such as temperature, emission angle, and wavelength.

Based on Stefan- Boltzmann law, the variable that would reduce the back radiated energy is the temperature difference between the asphalt pavement surface and ambient temperature (air). The hypothesis of this study is that the surface temperature of the asphalt pavement will be reduced due to the convective heat transfer of water flowing underneath it, which will decrease the back radiated energy emitted from asphalt pavement to the air.

Experimental work

In the first step three thermocouples were used for the temperature data collection from the surface one directly at the center, and other two 0.0254m (1") from the sample edge (Figure 5). This arrangement was made for four samples – two for Q mix and two for M mix. The samples were compacted in similar manner, using the same amount of asphalt binder. (Bulk specific gravity for Q mix= 2.208 and M mix= 2.265). Of the two samples made for each mix, one was fitted with a copper pipe approximately 1 inch below the surface to flow water through it.

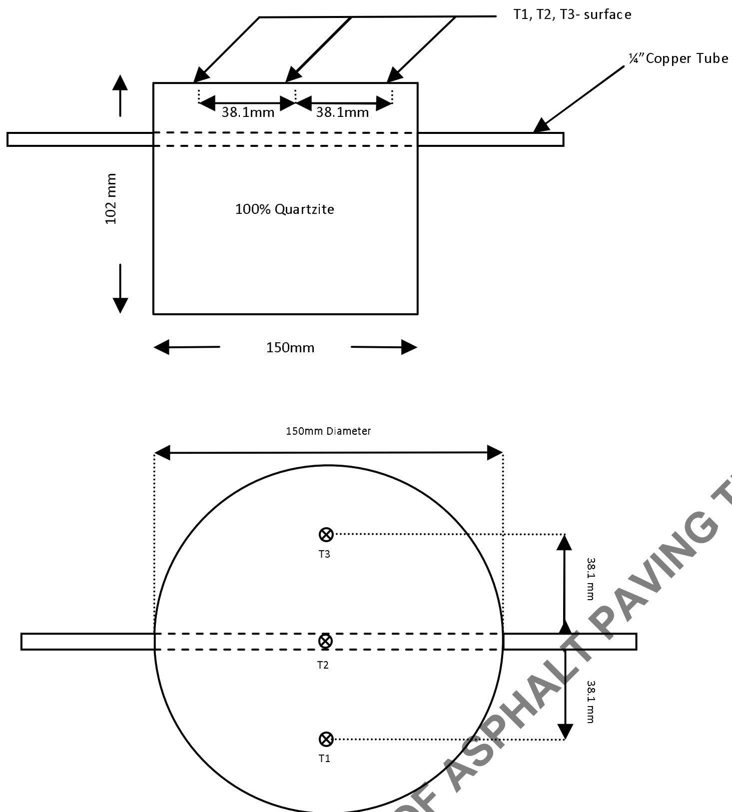

Figure 5 Samples with three thermocouples

For the samples without pipe, the lamp was left on for eight hours, and then switched off, and data were collected for the next eight hours; this procedure was repeated three times for each sample with 24 hours interval between two successive heating cycles.

For the sample with pipe, the lamp was left on for four hours, without flowing water, and water was flowed for four hours after which the lamp was switched off and the water was kept flowing for another four hours. This procedure was repeated three times for each sample with 24 hours interval between two successive heating cycles.

Plots of surface temperature versus time are shown in Figures 6 and 7. Figure 6 shows that the maximum temperature of the M mix is higher than the maximum temperature of the Q mix.

This is due to the higher thermal conductivity of the Q mix. Figure 7, in comparison to Figure 6, shows clearly that the maximum temperature reached in the two samples with water flow are significantly lower compared to those without any water flow.

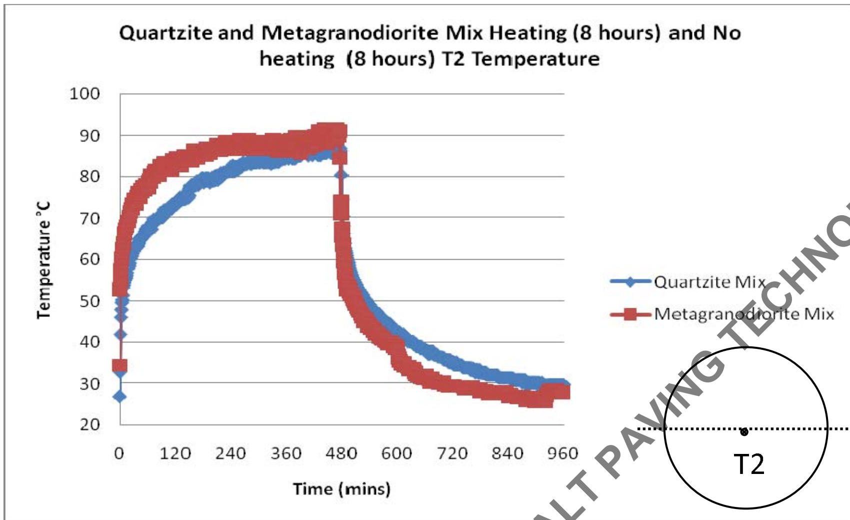

Figure 6 8-hour heating and 8-hour no heating data for surface temperature for quartzite and metagranodiorite mixes

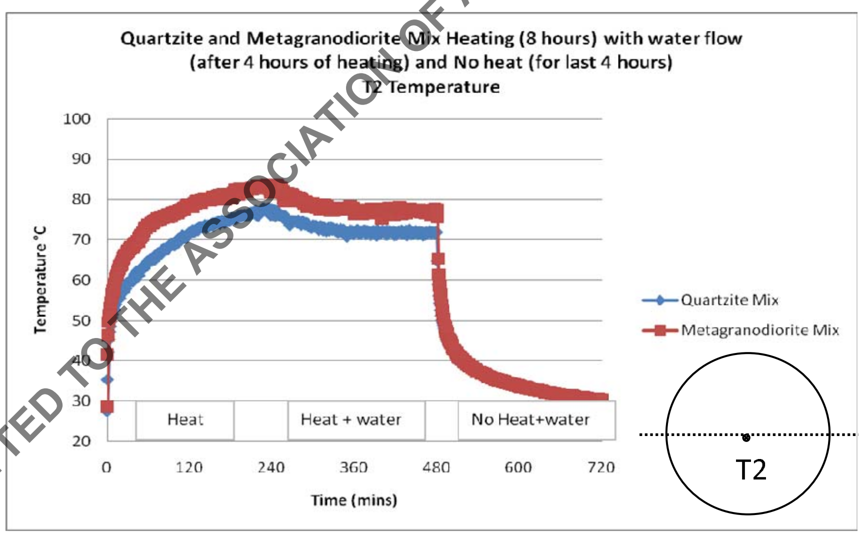

Figure 7 Heating with water flow data for surface temperature for quartzite and metagranodiorite mixes.

In the next step, a detailed investigation of the quartzite samples only was conducted, using seven thermocouples for each sample, as shown in Figure 8.

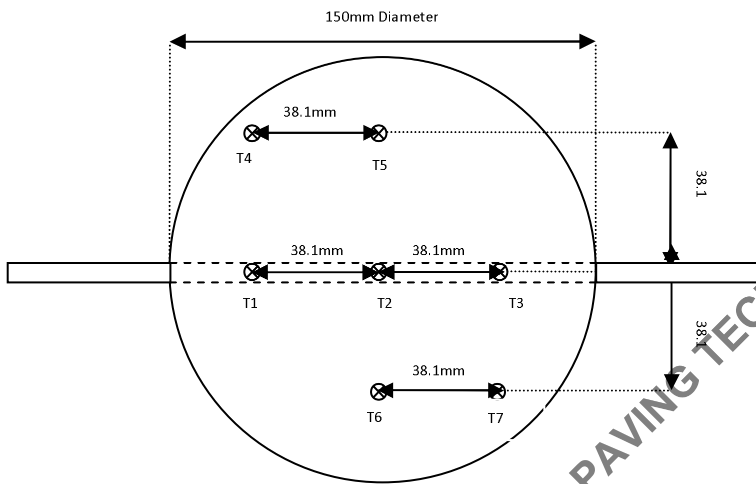

Figure 8 Layout of thermocouples for next set of experiments

The following plots (Figure 9) show the temperature versus time data for each of the seven thermocouples (T1 through T7) on the surface, for the case where the sample was heated for 8 hours and then not heated for the next 8 hours (designated as 8/8 hrs), and the case for which the sample was heated for 8 hours, where water was flowed after the first 4 hours of heating and then not heated for 4 hours (designated as 4/4/4 hrs).

All of the plots, except the one for the T7 thermocouple, show that there is a significant reduction in surface temperature of the sample as a result of flowing water. They also show that at the end of the heating period, the cooling rate is higher for the samples that have water flowing through them.

The results are more prominent for the T1, T2 and T3 thermocouples, which are at the center line of the sample and fall immediately above the copper pipe carrying water inside the sample.

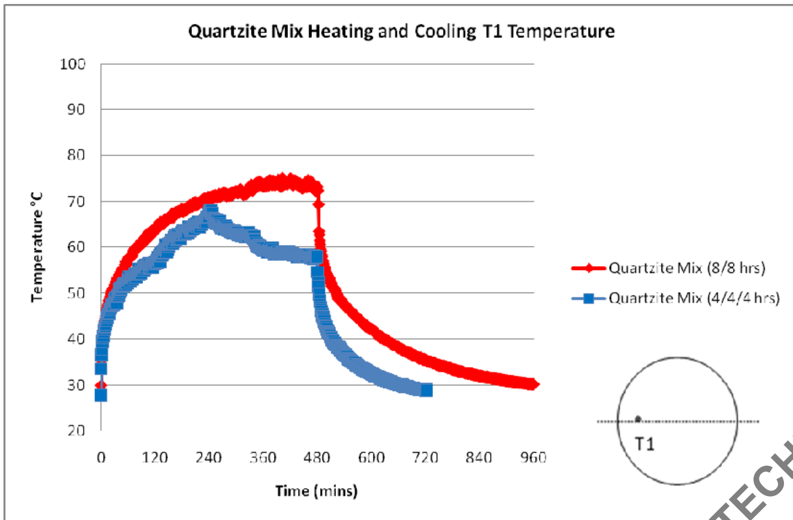

Figure 9 Plots of time versus temperature

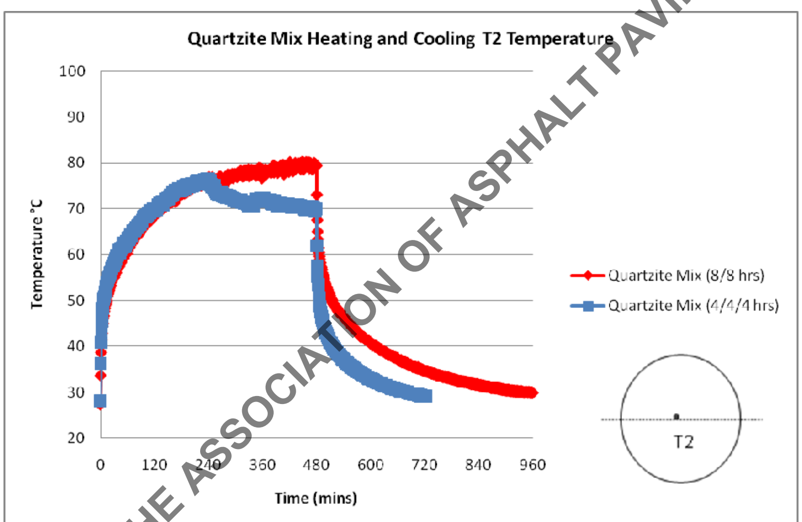

Figure 9 Plots of time versus temperature (continued)

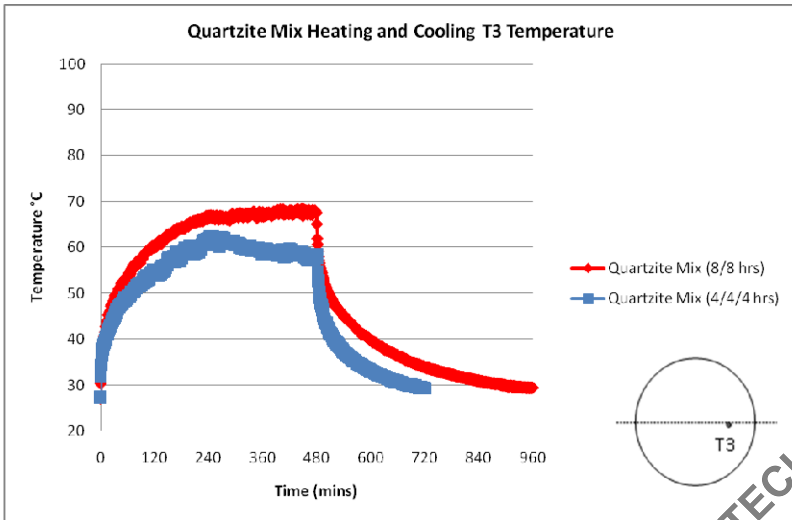

Figure 9 Plots of time versus temperature (continued)

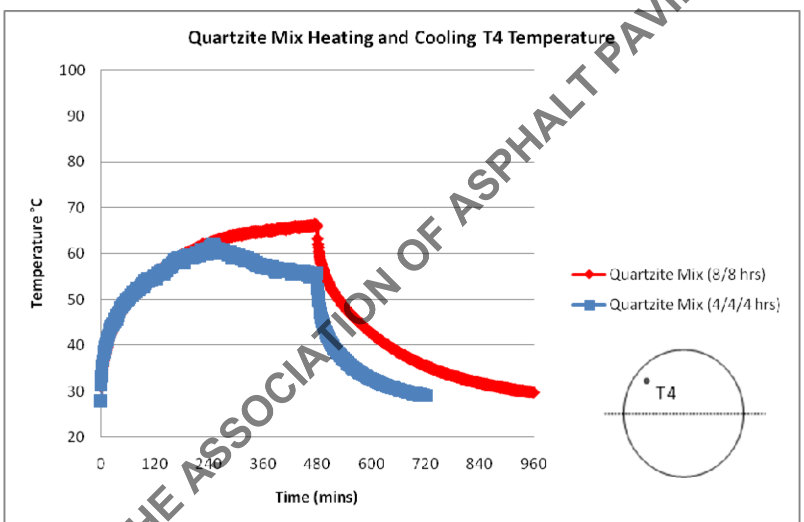

Figure 9 Plots of time versus temperature (continued)

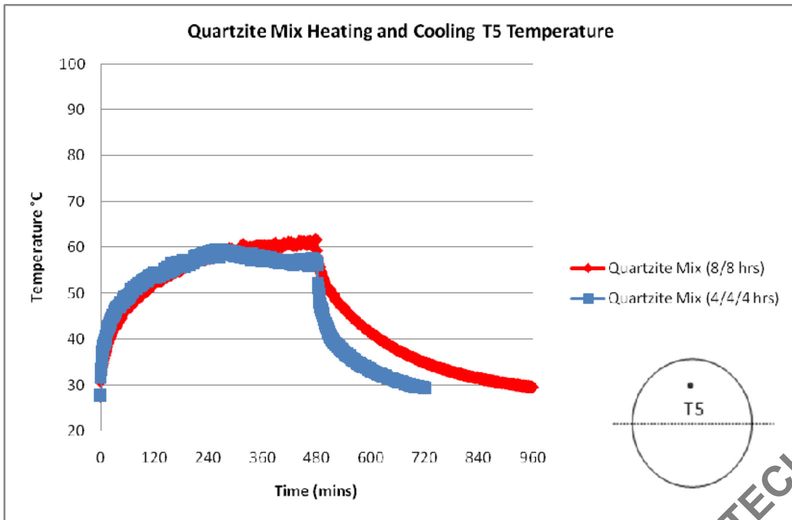

Figure 9 Plots of time versus temperature (continued)

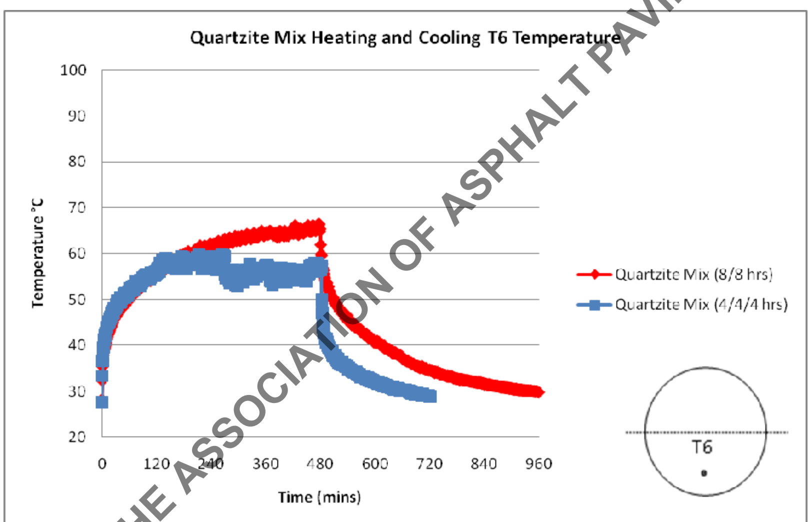

Figure 9 Plots of time versus temperature (continued)

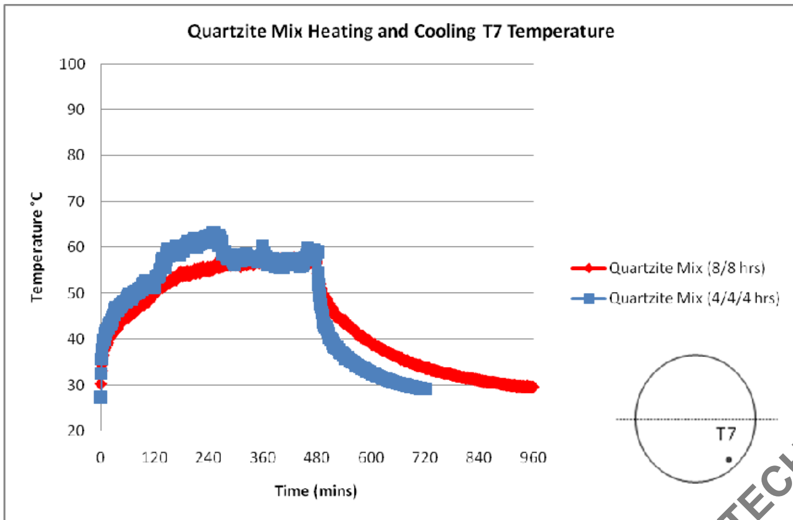

Figure 9. Plots of time versus temperature (continued)

Note that the filament of the halogen lamp operates at very high temperature and delivers a "cone" heat flux onto the sample surface. The thermocouples on the sample surface are very sensitive to the position of the halogen lamp; this causes slight variation in temperature measurement (as seen for T7).

Table 1 shows the average reduction of temperature for the different locations on the sample.

Table 1 Average Reduction in surface temperature due to flowing water

Thermocouple	T1	T2	T3	T4	T5	T6	T7
Max	70.83	76.77	61.30	66.98	64.31	61.71	57.12
Min	57.40	72.09	56.33	57.32	58.94	55.69	55.10
ΔT (°C)	13.43	4.68	4.96	9.65	5.37	6.02	2.02

Note: The position of T2 is right underneath the halogen filament and the measured temperature is always slightly higher

From the various plots in Figure 9 it can be seen that for the first 4 hours all thermocouples showed similar rise in temperature; however when water was turned on thermocouples T1-T6 show lower temperature over the next four hours. The mean drop of temperature (ΔT) was 13.43 °C for T1 because its location is near the pipe (water) entrance region which had the coldest water (25.5 °C) that led to the largest drop in temperature. The effect seems to taper off in the midsection by T2 and also in the tail-end section (T3). The other prominent effect was the significant lowering of temperature at T4 which is placed 38.1 mm from the centerline of the pipe. The temperature at this location fell by almost 10 °C. The numbers steadied to between 5 and 6 °C in the midsection at these far locations (38.1mm). Results indicate that the cooling potential of water flowing through a pipe can radially extend for almost 40 mm.

To evaluate the effect of increased surface area of pipe on the drop in temperature, experiments were conducted with pipes of serpentine (S) shape (Figure 10), so as to cover more area of the HMA sample. The plots for the experimentally obtained data for the 28 inch serpentine pipe for T1-T7 are shown in Figure 11. The results clearly show the higher reduction of surface temperature for the S pipes compared to the straight pipe.

Figure 10 Serpentine pipe in a sample (during compaction)

17

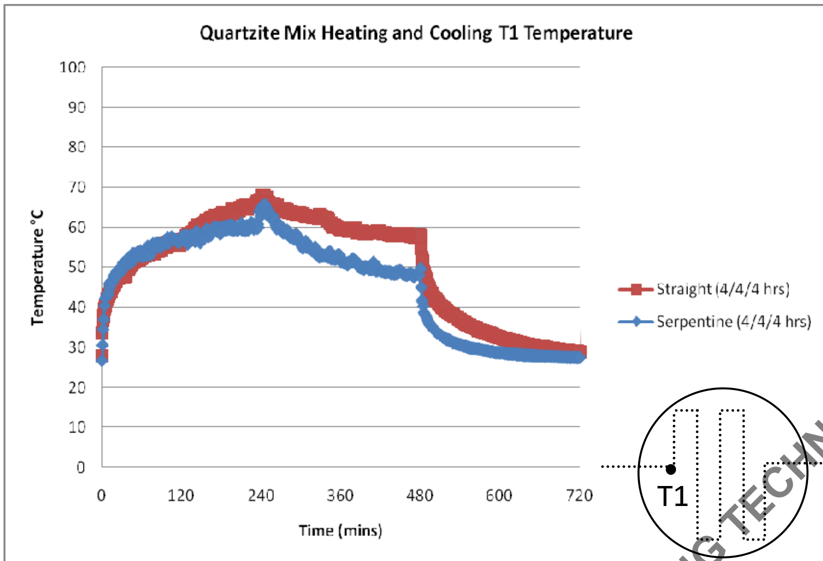

Figure 11 Plots of time versus temperature

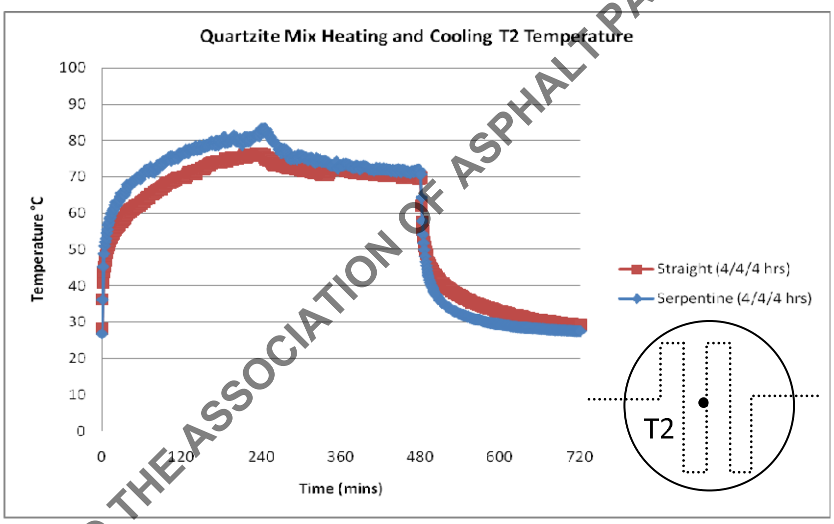

Figure 11 Plots of time versus temperature (continued)

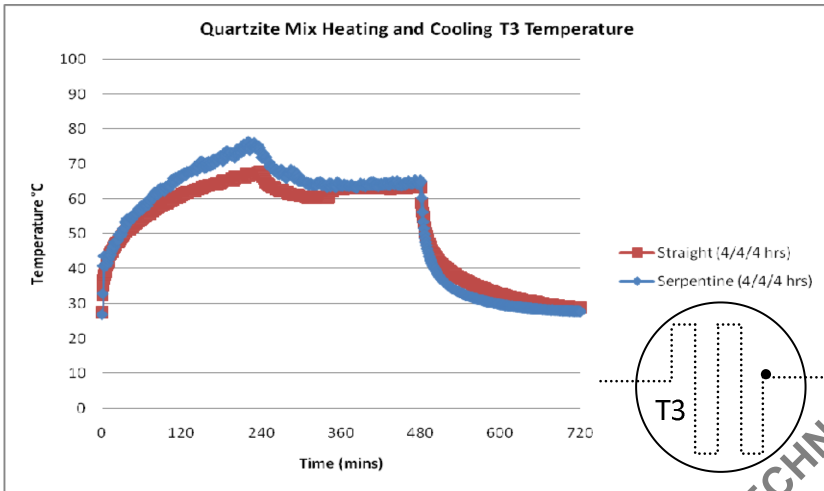

Figure 11 Plots of time versus temperature (continued)

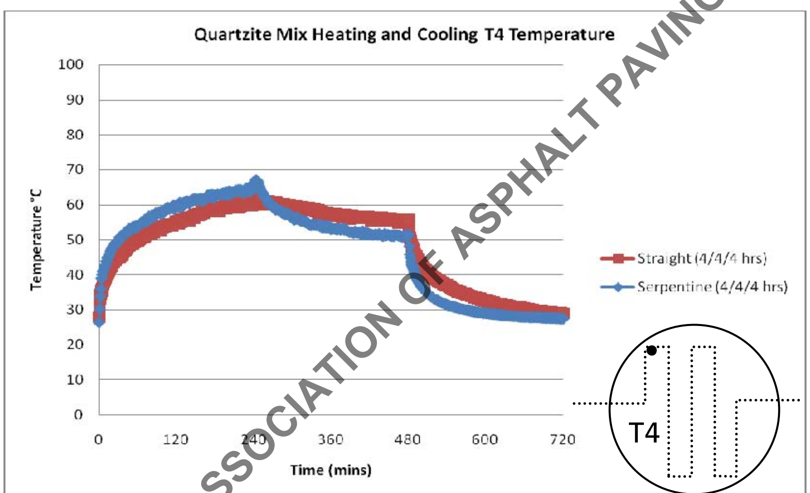

Figure 11 Plots of time versus temperature (continued)

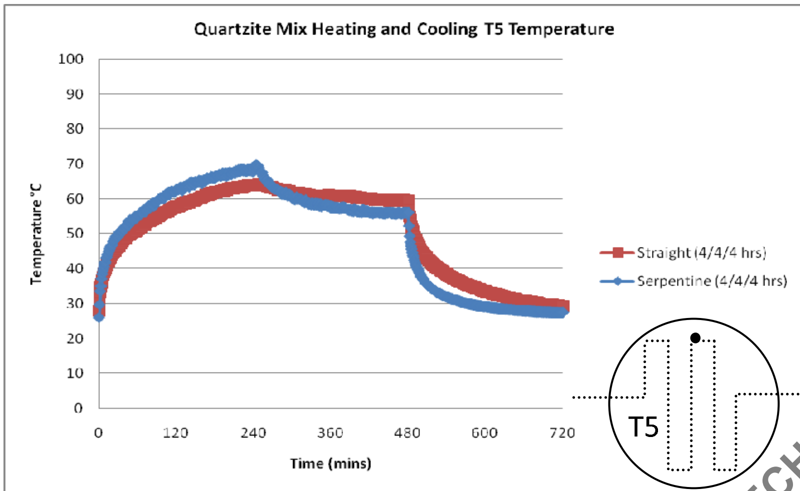

Figure 11 Plots of time versus temperature (continued)

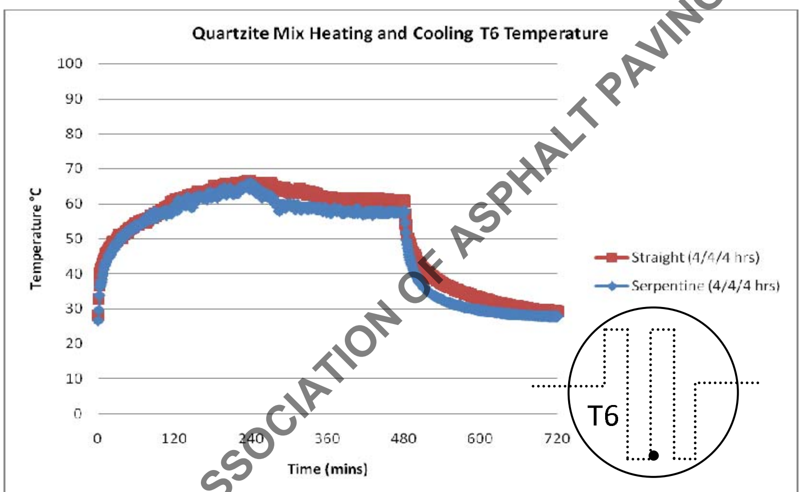

Figure 11 Plots of time versus temperature (continued)

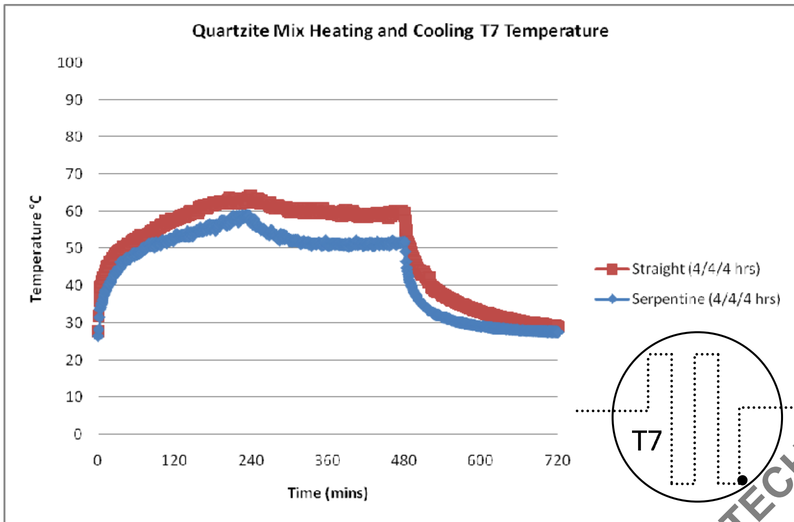

Figure 11 Plots of time versus temperature (continued)

Understand the Effect of Important Factors

The more the heat can be transmitted away from the pavement, the less will be the difference between the surface and air temperature and hence less will be the heat radiated back into the atmosphere. Hence, the most rational way to minimize the urban heat island effect is to maximize the transfer of heat away from the pavement. As indicated in Figure 12, this process involves two important steps- a) Maximizing the heat extraction from the pavement in the piping network and b) Absorbing the maximum solar radiation in the pavement.

The rest of the paper presents results of work that was conducted to explore step a), as mentioned above

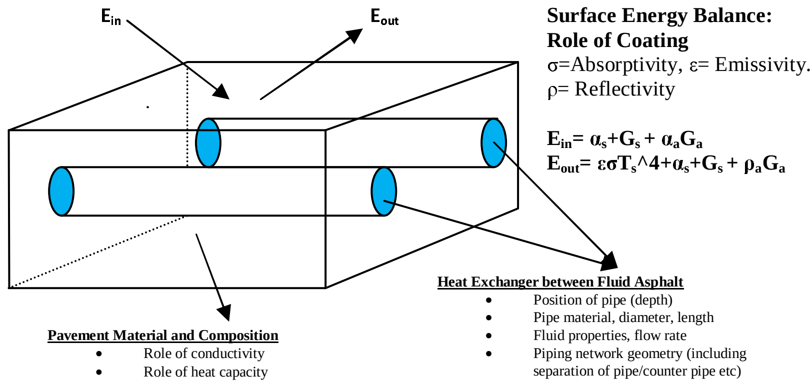

Figure 12 Different important components of the heat exchange process from pavements

Note that efficiency is defined as

$$E = \frac{MC(T_{out} - T_{in})}{GA}$$

Where, E is efficiency, M is mass flow rate of water, kg/s, C is specific heat of water, J/kg·K, T_{out} is temperature of outgoing water, or final temperature of water in a bath, °C, T_{in} is temperature of incoming water, or initial temperature of water in a bath, °C, G is radiation, W/m^2, A is area of heat conduction (pi*pipe diameter*length of pipe inside HMA), m^2. Everything else remaining constant, E is therefore directly proportional to the difference in temperature between initial and final water temperature or between incoming and outgoing water (delta T), which was used in the subsequent analysis as the indicator of efficiency.

Temperature Profile in Water

The optimum heat transfer condition is achieved when the temperature of the heat exchanger fluid (water, in this case) reaches the temperature of the asphalt pavement at that depth. Analytical work was conducted to explore the temperature distribution within the water at different lengths from the inlet point.

This investigation was carried out using FE. For using FE to explore the temperature distribution, one needs to understand the velocity profile in the pipe. An uniform velocity profile was assumed. The velocity profile of the fluid U, can be identified and calculated based on the Reynolds's number and Power Law of Velocity (22).

Laminar flow ≤ Re = 2300

$$U = V_{max}\left(1 - \left(\frac{r}{R}\right)^2\right)$$

Turbulent flow ≥ Re = 2300

$$U = V_{max}\left(1 - \left(\frac{r}{R}\right)^7\right)$$

Where V_{max} is maximum velocity, r is any point at the diameter of pipe, and R is the radius of the pipe.

The fully developed flow and uniform velocity profile were assumed to minimize the velocity variation at the entrance region and the boundary layer, which increased the stability of the problem of heat transfer and water temperature distribution/profile in the copper pipe in the FE analysis.

The heat transfer module of COMSOL (20) was used to simulate the problem, and the resultant temperature profiles are shown in Figures 13 and 14.

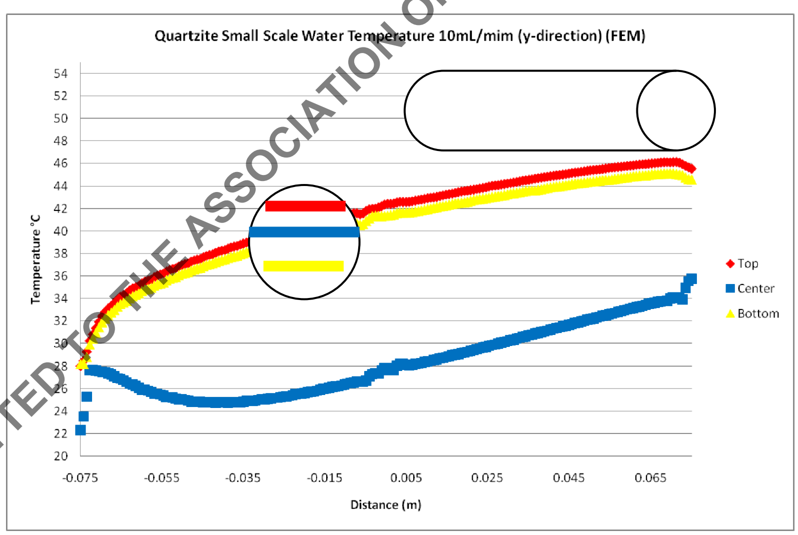

Figure 13 Temperature in pipe along the length

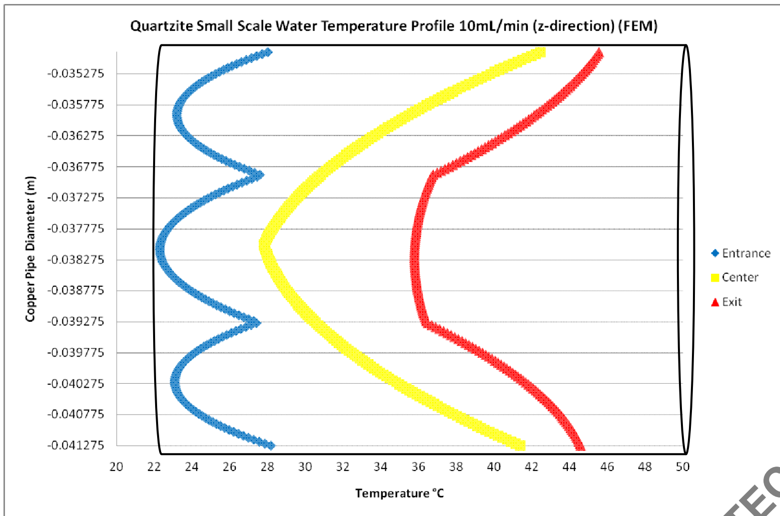

Figure 14 Temperature across the pipe

Then, theoretical calculations were made to determine the length of the pipe needed for specific diameter and flow rates, to achieve the maximum temperature.

The value of the convection heat transfer coefficient for internal flow is dependent on the geometrical cross section of the pipe, the thermal boundary condition at the pipe wall, and the distance at pipe entrance. The Nusselt number is defined as

$$Nu = \frac{hd_h}{k}$$

Where d_h is the hydraulic diameter of the section, h is the heat transfer coefficients and k is the thermal conductivity of the fluid.

There are two types of boundary conditions used in convection heat transfer, uniform wall flux and uniform wall temperature.

Uniform wall flux $\dot{q}_w''$ is when the heat flux at the wall of the pipe is uniform,

$$T_b = \frac{\dot{q}_w'' A}{\dot{m} C_p} + T_i$$

$$\dot{q}_w'' = h_x(T_w - T_b)$$

Where T_b is the exit temperature, A is the surface area of the pipe, $\dot{m}$ is the mass flow rate, C_p is heat capacity, T_i is the initial temperature at the entrance, h_x is the local heat transfer coefficient, and T_w is the wall temperature.

Uniform wall temperature is when the temperature at the wall is uniform; the local heat flux is replaced by $h_x(T_w - T_b)$, the equation (23) can be rearranged as

$$\frac{T_w - T_b}{T_w - T_i} = exp\left[-\frac{\bar{h}A}{\dot{m}C_p}\right]$$

Where $\bar{h}$ is the average heat transfer coefficient.

For circular pipe, the typical Nusselt numbers for fully developed flow are 4.36 and 3.66 for Uniform Heat Flux and Uniform Wall Temperature, respectively.

Prior experiments (19) showed that the maximum average temperature below 0.0254m (1”) of the asphalt pavement surface was approximately 50 °C (for the case studied). This value was then used (as an example) as uniform wall temperature to calculate the effective copper pipe length with various pipe diameter and water flow rate. The results are shown in table 2. The results for asphalt mix temperatures of 40, 50 and 60^{o}C are shown graphically in Figure 15.

Table 2 Required pipe length for wall temperature= 50 °C

	Water Flow Rate (mL/min)							
Pipe Diameter (m)	100	200	400	600	800	1000	2000	4000
0.005	7.5	15	30	45	60	75	150	300
0.01	7.5	15	30	45	60	75	150	300
0.02	7.5	15	30	45	60	75	150	300
0.03	7.5	15	30	45	60	75	150	300
0.04	7.5	15	30	45	60	75	150	300
0.05	7.5	15	30	45	60	75	150	300
0.06	7.5	15	30	45	60	75	150	300
0.07	7.5	15	30	45	60	75	150	300
0.08	7.5	15	30	45	60	75	150	300
0.09	7.5	15	30	45	60	75	150	300
0.1	7.5	15	30	45	60	75	150	300
	Pipe length (m)							

*turbulent flow cases highlighted

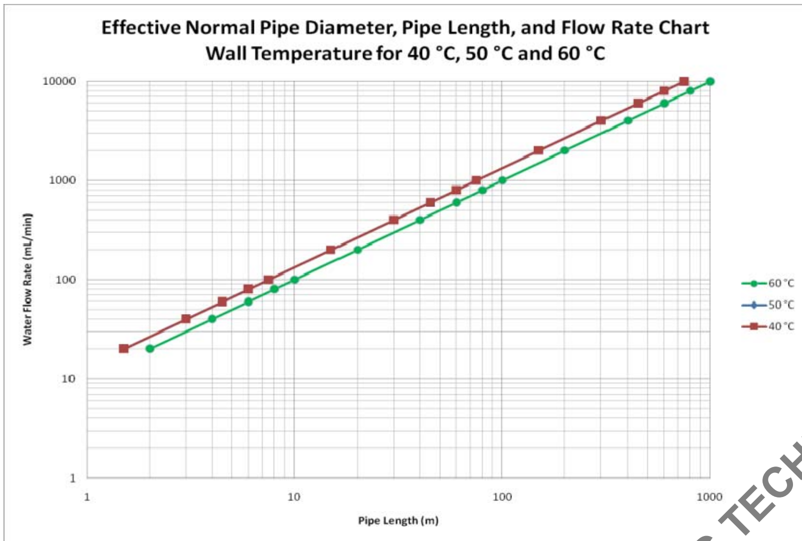

Figure 15. Plots for wall temperature of 40°C, 50°C and 60°C (40°C and 50°C are overlapped)

The heat transfer coefficient is inversely proportional to the hydraulic diameter (wet perimeter of pipe diameter), therefore, the smaller diameter of pipe resulted in highest heat transfer coefficient and required shorter length to achieve the wall temperature. In contrast, the larger diameter of copper pipe required longer length.

The effect of pipe (carrying water) spacing on asphalt mix temperature was analyzed by using FE, and this analysis helped us to visualize the formation of low temperature zone between pipes. Various pipe diameters were used, with the pipe spacing ranging from 0.0254m (2") to 0.6096m (24"). The results are shown in Figure 16, with an example model from FE analysis in Figure 17. This figure clearly shows the cooling effect of the more closely spaced pipes.

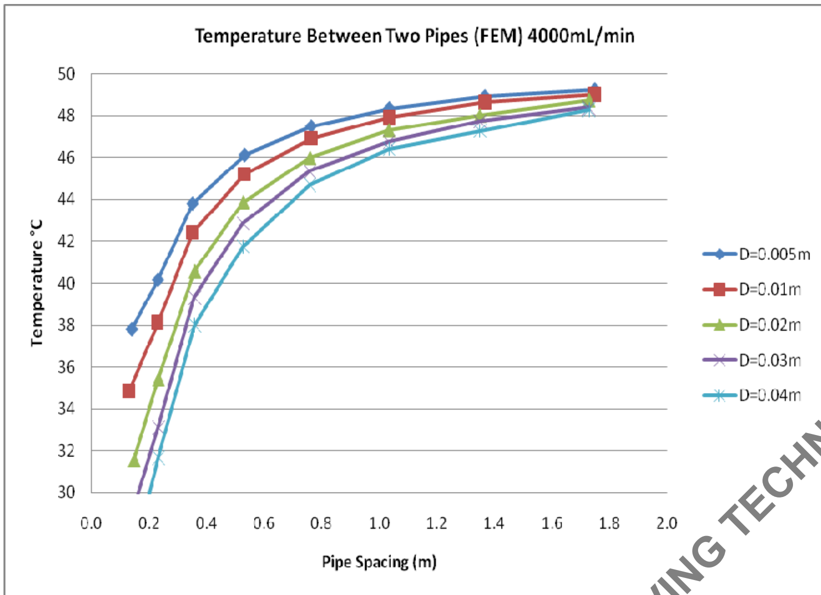

Figure 16 Plots of pipe spacing versus temperature for different diameters

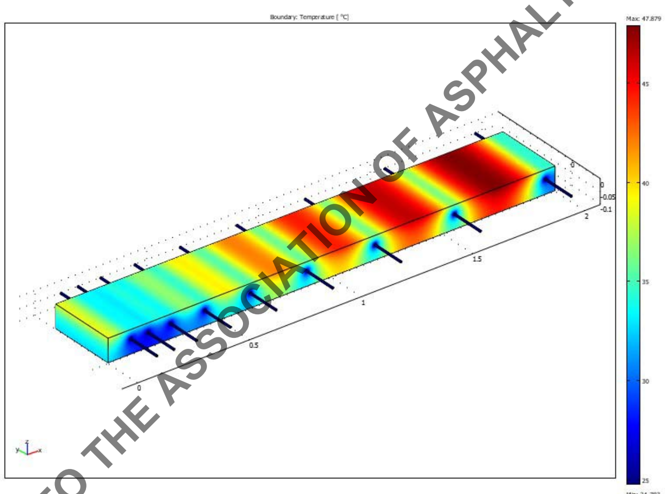

Figure 17 FE simulation for pipe spacing

Note that the slower flow rate (laminar flow) resulted in lower termperature variation between the pipes, when the pipe spacing were equal to 0.3556m (14") and 0.4064m (16"), - the temperature variation was minimal. The overall heat transfer coefficient is decreased in laminar flow and the temperature drop between pipes is reduced. On the other hand, the overall heat transfer coefficient is increased when tubulent flow occurrs and this results in higher temeprature drop between two pipe.

Since the actual length of pipe is limited, and it cannot be provided as a straight section, 3 different scenarios of pipe layout were analyzed by using the FE simulation, (1) 0.1524m (6") straight pipe, (2) 0.3556m (14") serpentine style pipe, and (3) 0.7112 (28") serpentine style pipe. The boundary conditions were assumed to be constant temperature (based on experimental data) along the interface with asphalt sample and thermally insulated at other surface; 10mL/min water flow rate (fully developed laminar flow) was used as water velocity; in actual experiment the temperature of the pipe is not constant along the diameter of the sample, since because of the entering cold water, the pipe part near the inlet will be at a lower temperature than the remaining part; this could at least partially explain the difference between FE (higher) and the lab delta Ts.

The results of the FE analysis (Figure 18) clearly show the higher temperature of the water for the serpentine pipes as compared to the straight pipe.

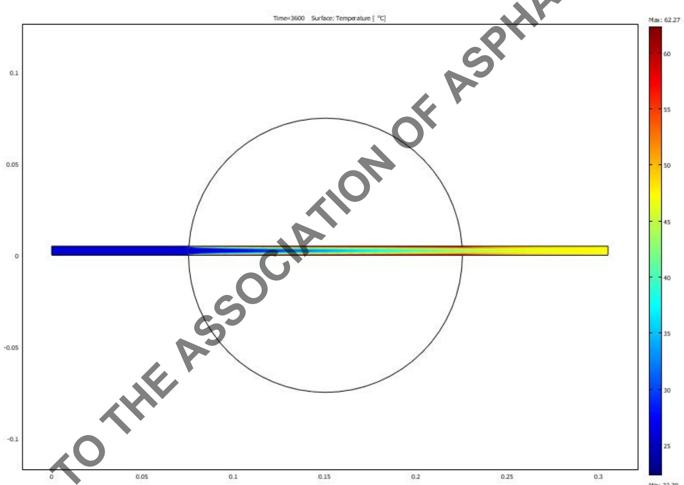

Figure 18 Temperature distribution in different shaped pipes (6" straight pipe)

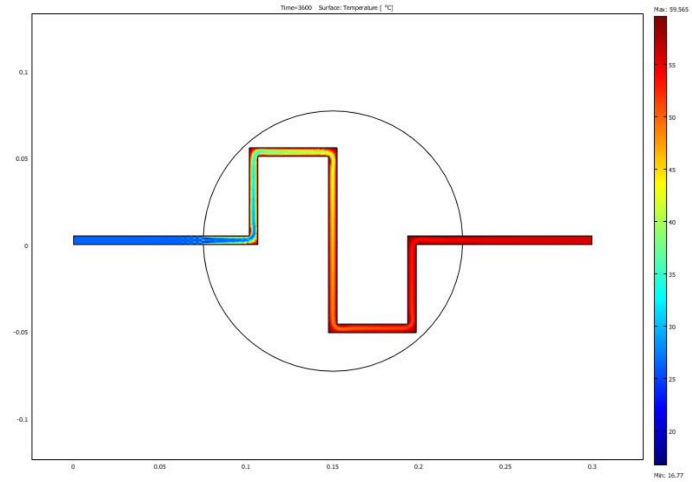

Figure 18 Temperature distribution in different shaped pipes (14”serpentine pipe) (continued)

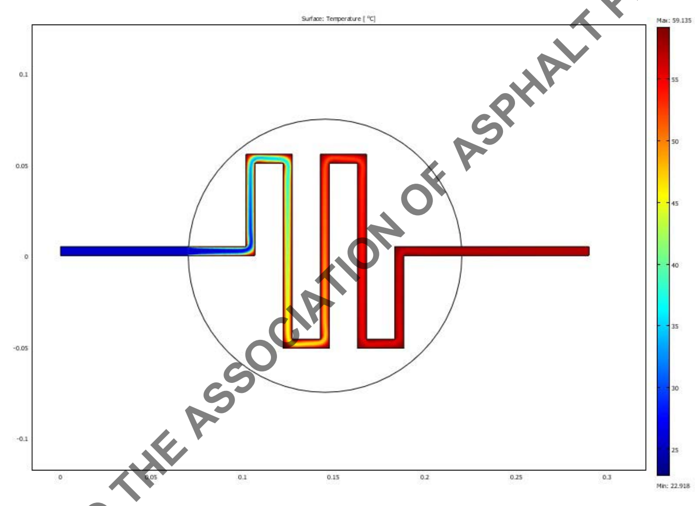

Figure 18 Temperature distribution in different shaped pipes (28”serpentine pipe) (continued)

Experiments were carried with S pipes to validate the FE analysis. The results from both experiments and FE analysis (in terms of delta T, that is difference between out let and inlet water temperature) are shown in Table 3.

Table 3 Water temperature comparison

	Quartzite Mix 10mL/min at 60mins	
	LAB ΔT	FEM ΔT (2D Analysis)
6" Straight Pipe	11.21	20.65
14" Serpentine Pipe	19.76	28.35
28" Serpentine Pipe	27.13	33.25

The laboratory results showed that the pipe with larger surface area yielded higher temperature at the exit. When the pipe length increased from 0.1524m (6") to 0.3556m (14"), the temperature resulted in approximately 8.55°C difference; when the pipe length increased from 0.3556m (14") to 0.7112m (28"), the temperature increased approximately by 7.37°C, which meant that the large surface area of pipe yielded higher temperature, but the efficiency of the process decreases with an increase in the temperature of water in the pipe.

The effective pipe length is relative to pipe diameter, water flow rate, and wall temperature; these factors are needed to be taken into consideration when designing the pipe layout.

Difference between Predicted and Observed Delta T

Note that, significant differences were obtained between laboratory test results and FEM predictions (from 3-D analysis, as shown in Figure 19) for samples in which the pipe was inserted after drilling a hole through the compacted sample (Table 4). It was hypothesized that this occurred because the pipes were not in good contact with the mix. Another set of samples were then compacted using a procedure in which the pipe was laid down during compaction (as would be expected in the field).

The results from these samples (Table 5) showed much lower difference from those predicted from the models, confirming the importance of the compaction process and the necessity to ensure maximum contact between the sample and the pipe.

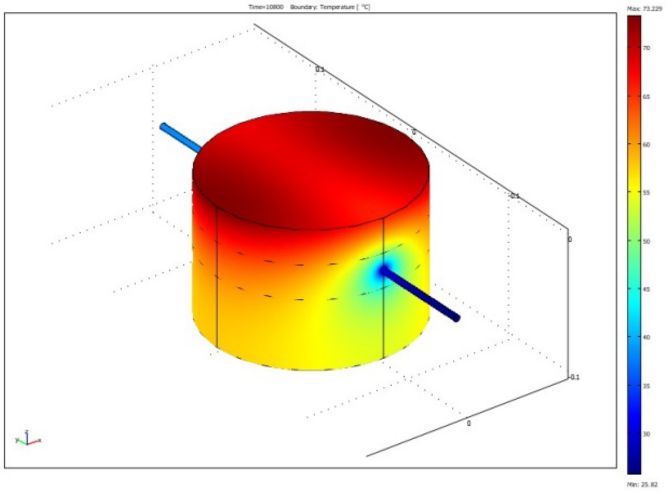

Figure 19 Model for 3-Dimensional FE analysis

Table 4 Temperature difference at time= 60 minutes, with water, 10 ml/minute, for samples in which the pipe was placed in a drilled hole in the compacted sample

	Lab ΔT, °C	FE ΔT, °C (3DAnalysis)
100% Metagranodiorite Mix	7.22	14.61
100% Quartzite Mix	8.62	15.20

Table 5 Temperature difference at time= 60 minutes, with water, 10 ml/minute, for samples in which the pipe was placed during compaction of the sample

	Lab ΔT, °C	FE ΔT, °C (3D Analysis)
100% Metagranodiorite Mix	9.87	13.91
100% Quartzite Mix	11.21	15.91

Although the difference between the test results and the FE were reduced, most likely by the better contact between the asphalt mix and the pipe, some difference still remained. Reasons for the remaining difference between experimental and model values could be one or more of the following:

- Fully developed laminar flow (velocity profile) is assumed in analysis but cannot be fully developed in experiment ;
- Overall thermal conductivity and heat capacity were back-calculated based on temperature distribution of sample and 10% error was allowed;

- The FE analysis assumed a homogeneous material for the sample.

Conclusions and Recommendations

Based on the results of this study, the following conclusions can be made:

1. It is possible to lower the surface temperature of asphalt pavements by flowing water underneath the pavement.
2. The reduction in temperature is affected by the type of conductivity of the mix – higher the conductivity, higher is the reduction temperature.
3. The process of reduction in temperature can be optimized by the maximum extraction of heat from the pavement through a fluid.
4. The amount of heat that can be extracted depends on the surface area of the pipes carrying the fluid.
5. Serpentine pipes can be used to improve the efficiency of heat transfer by providing larger surface area.
6. Better contact between the pipe and the pavement mix would lead to improved efficiency of heat transfer.
7. Further studies are needed with different pipe geometries and spacing to optimize a system of reducing the heat island effect and using the heat energy for end application.

Acknowledgement

The authors are deeply grateful to Mike Hulen and Cameron Feldman of Novotech Inc, for their guidance and encouragement, and Ron Tardiff of Aggregate Industries and Jeff Carlstrom of New Ulm Quartzite Quarries for providing the materials. This study would not have been possible without the laboratory and shop help from Yanxuan Xiu, Karen O'Sullivan, Don Pellegrino and Dean Daigneault of the Civil and Environmental Engineering department at Worcester Polytechnic Institute (WPI).

References

1. The United States Environmental Protection Agency, "Heat Island Effect", http://www.epa.gov/hiri/
2. Martina Soderlund, Stephen T. Muench, Kim A. Willoughby, Jeffrey S. Uhlmeyer, Jim Weston, "Green Roads: A Sustainability Rating System for Roadways" Transportation Research Board 87th Annual Meeting, 2008
3. Mark Belshe, Kamil E. Kaloush, Jay S. Golden, Michael S. Mamlouk, Patrick Phelan, "Asphalt-Rubber Asphalt Concrete Friction Course Overlays as Pavement Preservation Strategy for Portland Cement Concrete Pavement" Transportation Research Board 86th Annual Meeting, 2007
4. H.F. Southgate, and R.C. Deen, "Temperature Distribution within Asphalt Pavements and its Relationship to Pavement Deflection" Transportation Research Record 291, Transportation Research Board, National Research Council, Washington, DC, 1969
5. Ake Hermansson, "Simulation Model for Calculating Pavement Temperatures Including Maximum Temperature" Transportation Research Record, No. 1699, Transportation Research Board, National Research Council, Washington, DC, 2000
6. Donh-Yeob Park, Buch,Neeraj, Chatti Karim, "Effective Layer Temperature Prediction Model and Temperature Correction via Falling Weight Deflectometer Deflections" Transportation Research Record, No. 1764, Transportation Research Board, National Research Council, Washington, DC, 2001
7. C. K. Yavuzturk, Ksaibati, A.D. Chiasson, "Assessment of Temperature Fluctuations in Asphalt Pavements Due to thermal Environment Conditions Using a Two Dimensional, Transient Finite-Difference Approach" Journal of Materials in Civil Engineering, ASCE Volume 17, Issue 4, July/August 2005
8. M. Solaimanian, T.W. Kennedy, "Predicting Maximum Pavement Surface Temperature Using Maximum Air Temperature and Hourly Solar Radiation" Transportation

Research Record, No. 1417, Transportation Research Board, National Research Council, Washington, DC, 1993.

9. G. A. Huber, "Strategic Highway Research Program Report SHRP 648A: Weather Database for the Superpave Mix Design System" Transportation Research Board, National Research Council, Washington, DC, 1994.
10. M. Solaimanian, P. Bolzan, "Strategic Highway Research Program Report SHRP –A-637: Analysis of the Integrated Model of Climate Effects on Pavements" Transportation Research Board, National Research Council, Washington, DC, 1993.
11. K. Brian Diefenderfer, Imad L. Al-Qadi, D. Stacey, "Model to Predict Pavement Temperature Profile" The Journal of Transportation Engineering, ASCE, Vol. 132, No. 2, February 1, 2006.
12. Donath Mrawira, Joseph Luca, "Thermal Properties and Transient Temperature Response of Full-Depth Asphalt Pavements" Transportation Research Record, No. 1809, Transportation Research Board, National Research Council, Washington, DC, 2002.
13. Joseph Luca, Donath Mrawira, "Solar-Convection Simulator for Laboratory Investigation of Transient Temperature Fluctuations in HMAC Pavements" 83rd Annual Meeting of the Transportation Research Board, Washington, DC, 2004.
14. Joseph Luca, Donath Mrawira, "New Measurement of thermal Properties of Superpave Asphalt Concrete" Journal of Materials in Civil Engineering ASCE Volume 17, Issue 1, (January/February 2005).
15. M. Hasebel,Y. Kamikawa, and S. Meiarashi "Thermoelectric Generators using Solar Thermal Energy in Heated Road Pavement" 2006 International Conference on Thermoelectrics, IEEE.
16. Heat Island Group, "Learning about Urban Heat island" http://eetd.lbl.gov/HeatIsland/LEARN/
17. Kanok Boriboonsomsin, Farhad Reza, "Mix Design and Benefit Evaluation of High Solar Reflectance Concrete for Pavements" Transportation Research Record: Journal of the Transportation Research Board No. 2011. 2007.

18. Bao-Liang Chen, Laura Rockett, Rajib B. Mallick, "A Laboratory Investigation of Temperature Profiles and Thermal Properties of Asphalt Pavements with Different Subsurface Layers" Journal of the Association of Asphalt Paving technologists, Volume 77, 2008 (in press).
19. Rajib B. Mallick, Bao-Liang Chen, Sankha Bhowmick, Michael Hulen, "Capturing Solar Energy from Asphalt Pavements" International Symposium on Asphalt Pavements and Environment, International Society for Asphalt Pavements, Zurich, Switzerland, 2008.
20. COMSOL. "Heat Transfer Module User's Guide." COMSOL Multiphysics 3.2.
21. Christoph Clauser, Ernst Huenges, "Thermal Conductivity of Rocks and Minerals." American Geophysical Union, 1995.
22. Bruce R. Munson, Donald F. Young, Theodore H. Okiishi, "Fundamentals of Fluid Mechanics" 5th edition, John Wiley & Sons, 2005
23. Adrian Bejan, "Heat Transfer." John Wiley & Sons, 1993.